

Review

A Comprehensive Review of the Applications of Hierarchical Zeolite Nanosheets and Nanoparticle Assemblies in Light Olefin Production

Pannida Dugkhuntod and Chularat Wattanakit *

Department of Chemical and Biomolecular Engineering, School of Energy Science and Engineering, Nanocatalysts and Nanomaterials for Sustainable Energy and Environment Research Network of NANOTEC, Vidyasirimedhi Institute of Science and Technology, Rayong 21210, Thailand; s15_pannida.d@vistec.ac.th

* Correspondence: chularat.w@vistec.ac.th; Tel.: +66-3-301-4255

Received: 28 January 2020; Accepted: 12 February 2020; Published: 18 February 2020



Abstract: Light olefins including ethylene, propylene and butylene are important building blocks in petrochemical industries to produce various chemicals such as polyethylene, polypropylene, ethylene oxide and cumene. Traditionally, light olefins are produced via a steam cracking process operated at an extremely high temperature. The catalytic conversion, in which zeolites have been widely used, is an alternative pathway using a lower temperature. However, conventional zeolites, composed of a pure microporous structure, restrict the diffusion of large molecules into the framework, resulting in coke formation and further side reactions. To overcome these problems, hierarchical zeolites composed of additional mesoporous and/or macroporous structures have been widely researched over the past decade. In this review, the recent development of hierarchical zeolite nanosheets and nanoparticle assemblies together with opening up their applications in various light olefin productions such as catalytic cracking, ethanol dehydration to ethylene, methanol to olefins (MTO) and other reactions will be presented.

Keywords: hierarchical zeolites; zeolite nanosheets; nanoparticle assemblies; light olefins

1. Introduction

Light olefins including ethylene, propylene and butylene are one of the most important chemical building blocks, which are widely used as precursors for many products in petrochemical industries such as polyethylene, polypropylene, acrylonitrile and propylene oxide. Typically, ethylene and propylene are produced via various processes such as steam cracking, fluid catalytic cracking (FCC) and on-purpose processes [1]. Among them, a high portion of light olefins has been produced via steam cracking, which requires severe conditions operated at a very high temperature (>850 °C), eventually yielding a high amount of methane and carbon dioxide as by-products [2,3]. In order to circumvent this problem, catalytic processes such as catalytic cracking and methanol to light olefins (MTO) are one of the most promising alternative routes for efficient light olefin production because of their lower operating temperature and a controllable product distribution.

Typically, heterogeneous catalysts are one of the most important ingredients in catalytic processes and one type of them, which has been widely used in light olefin production, is a zeolite. Due to the fact that it exhibits several outstanding and unique properties such as high surface areas, appropriate acid properties, shape selectivities, and thermal and hydrothermal stabilities, it can be used in many potential applications including adsorption, separation, ion-exchange and especially catalytic applications [4]. Zeolites are classified into various types of framework structures such as Zeolite Socony Mobil-five (MFI), chabazite (CHA), and zeolite beta (BEA). If they are considered by the size of pore opening

windows, they can be divided into three different categories including large porous, medium porous and small porous zeolites, which are composed of a different number of tetrahedral units, or T atoms of 12, 10 and 8 membered rings, respectively. These behaviors make each zeolite serving unique shape selective properties, which are very important for the appropriate applications.

Although there are several above-mentioned promising properties of zeolites, they are typically composed of a very small microporous structure, eventually resulting in some disadvantages of the diffusion limitation of guest molecules inside the framework. Some bulky molecules cannot easily penetrate into active sites located at microporous channels, and therefore a poor catalytic performance due to a very low reaction rate and a fast deactivation of catalysts is observed. To overcome these limitations and to improve the accessibility of molecules into active sites, in recent years modified zeolites obtained by introducing additional larger porous structures have been extensively developed [5–8].

It is well known that hierarchical zeolites, composed of at least two levels of porous structures such as micropores and mesopores, micropores and macropores, and micropores/mesopores and macropores have been extensively studied and developed. Their microporous (<2 nm), mesoporous (2–50 nm) and/or macroporous (>50 nm) structures are well connected to each other. In this case, the additional larger porous structures can improve diffusion limitation, molecular transportation and coke deposition [9]. In the past decade, there have been several studies regarding the synthesis of hierarchical zeolites to overcome these problems. Herein, this comprehensive review opens up perspectives of the recent synthesis approaches of hierarchical zeolite nanosheets and nanoparticle assemblies, as well as the successful production of light olefins via catalytic cracking, ethanol dehydration to ethylene, methanol to olefins (MTO) and other reactions.

2. Design of Hierarchical Zeolites

As stated above, there are many types of hierarchical zeolites which have been fabricated in recent years. This comprehensive review mostly focuses on the design of hierarchical zeolites with nanosheet structures and nanoparticle assemblies, as shown in detail below.

2.1. Synthesis of Hierarchical Zeolite Nanosheets

The first synthesis of MFI zeolite nanosheets was approached using the designed diquatery ammonium surfactant, $C_{22}H_{45}-N^+(CH_3)_2-C_6H_{12}-N^+(CH_3)_2-C_6H_{13}$ (denoted as C_{22-6-6}) as a structure-directing agent (SDA), which can be used to control microporous structures and nanolayer features [10]. MFI zeolite nanosheets exhibit a very high number of acid sites on the external surface, and high thermal/hydrothermal stability, which are appropriate for catalytic applications. The C_{22-6-6} surfactant was used, together with silica, for the synthesis of pillared MFI zeolite nanosheets. The silica pillars can generate mesopores in the interlamellar area of the zeolite nanosheets and the size of mesopore can be adjusted by the length of the hydrophobic tail using different sequence methods and synthesis time [11]. In this case, it is able to synthesize MFI nanosheets with a thin layer thickness (2 nm). Then, the restructuring process was further studied. It was found that the morphology of MFI nanosheets can be changed from a disordered assembly to an ordered multilamellar structure when increasing the hydrothermal aging time [12]. To control nanosheet structures, there are several types of surfactants, in particular, quaternary ammonium surfactants, as well as other templates or seeds that have been developed to synthesize various hierarchical zeolite nanosheets with different morphologies [13–15]. For example, tetrapropylammonium hydroxide (TPAOH) was used together with C_{22-6-6} as a dual-template to control hierarchical structures [13]. When increasing the amount of TPAOH, the morphology of the MFI nanosheet changes from intertwined particles to house-of-cards-structures. In addition, nanosheet HZSM-5 films deposited on the support and the hierarchical MFI nanosponge were successfully synthesized using C_{22-6-6} in seed-assisted synthesis methods [14,15]. Their hierarchical structures exhibit the remarkably improved activity attributing to the enhanced accessibility and diffusion of bulky molecules into the zeolite framework. Moreover, the multi-quaternary ammonium surfactants, composed of at least two ammonium groups, were also

applied for the hierarchical zeolite formation. Interestingly, the number of ammonium groups can also control the thickness of nanosheets. The further crystal growth can be suppressed by the micellar structure of surfactants with suitable long hydrophobic tails. However, the C/N^+ ratio of the terminated ammonium groups should not be too high for zeolite synthesis [16]. Other mixed templates such as [3-(trimethoxysilyl) propyl] hexadecyl dimethylammonium chloride [3-(trimethoxysilyl) propyl] hexadecyl dimethyl ammonium chloride [3-(trimethoxysilyl) propyl] hexadecyl dimethyl ammonium chloride (TPHAC)/tetrapropylammonium bromide (TPABr), diquatery ammonium/TPABr and diquatery ammonium/cetyltrimethylammonium bromide (CTAB)/TPAOH were applied to hierarchical zeolite nanosheet synthesis [17–19]. For example, the proposed mechanism for the formation of ZSM-5 nanosheets in the presence of C_{18-6-6} and TPABr is shown in Figure 1. In addition, single quaternary ammonium surfactants, which have π - π stacking of aromatic molecules in hydrophobic tails, were used as a template of MFI nanosheet synthesis. MFI nanosheets were self-assembled with perpendicular crystals and exhibited a high specific surface area in a mesoporous structure [20].

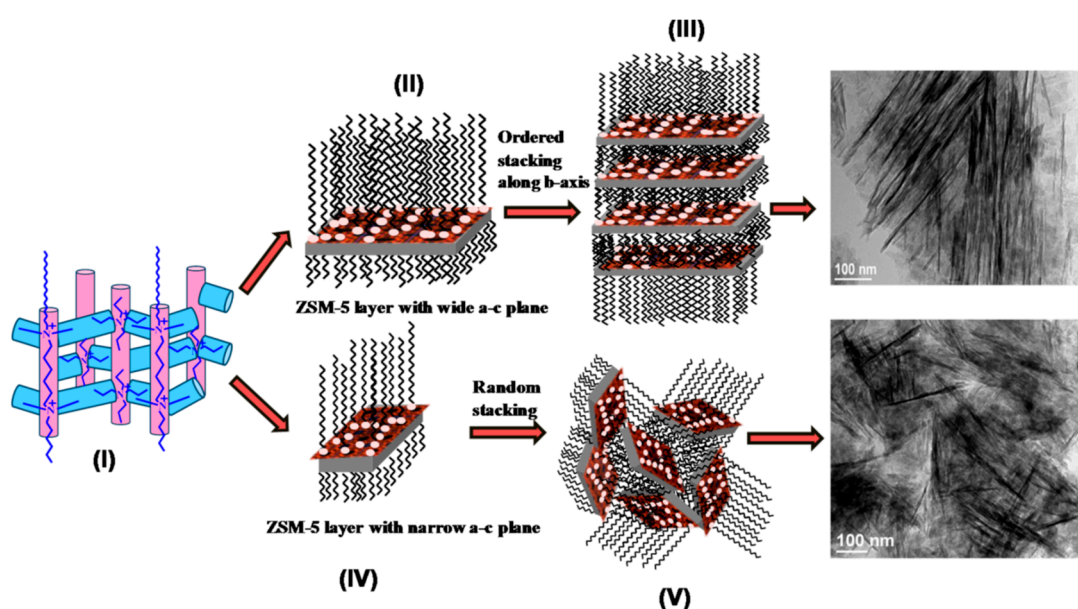


Figure 1. Proposed mechanism for the formation of ZSM-5 nanosheets in the presence of C_{18-6-6} and TPABr. Reprinted with permission from Reference [18]. Copyright 2018, American Chemical Society.

Furthermore, the bolaform tetra-head-group quaternary ammonium surfactant, composed of four quaternary ammoniums, a different length of alkyl chains and a rigid biphenol group, was used as a dual template to control both MFI zeolite frameworks and mesoporous structures. The ammonium headgroups interact with the alumina and silica parts of zeolite precursors to form MFI structures and the surfactant tails with a rigid biphenol group control the nanosheet structures. The morphologies and textural properties can be fine-tuned by the different bolaform structures [21]. However, the nanosheets morphology can be changed to house-of-cards structures, and then to nanosponges when decreasing the Si/Al ratios from 60 to 10, attributing to the systematical tailoring of their acidity and mesoporosity/microporosity [22]. Both an ammonium type surfactant and the tetra(n-butyl)phosphonium hydroxide solution (TBPOH) were used, forming a dual template. Not only an ammonium type surfactant but also the tetra(n-butyl)phosphonium hydroxide solution (TBPOH) was used alone as a dual template for the synthesis of MFI nanosheets with self-pillared nanolayer structures obtained via a one-step hydrothermal process, which is considered to be a new inexpensive procedure [23]. In addition, metals incorporated in MFI nanosheets can be synthesized with various metal decorations such as gallium [24,25]. The designed structures facilitate a short diffusion path length and high external surface area, eventually promoting the reaction of bulky molecules such

as long-chain alkanes and aromatics. In addition, ZSM-5 was synthesized by adding ZSM-5 seed with the $C_{18-6-6}Br_2$ template. Some parts of the ZSM-5 seed were dissolved to form nuclei and other parts acted as the core of epitaxial growth to facilitate nanosheet structures. The seed-fused ZSM-5 synthesis approach results in a short crystallization time, small particle size and the easy adjustment of surface acidities and textural properties [26]. Furthermore, siliceous nanosheets, which are representatives of the high silica zeolite, have also been developed. For example, phenylene-bridged hexagonally mesoporous organosilica with crystal-like walls (CW-Ph-HMM) was synthesized using 1,4-bis(triethoxysilyl)benzene (BTEB) as the organosilane precursor, and octadecyltrimethylammonium bromide (ODTMABr) as a structure-directing agent. The SEM images illustrate the nanosheet and nanofilament structures [27]. In addition, silica microcapsules with thin flake-shell structures were synthesized by a self-templating process. By adjusting the pH of the solution, the silanol-rich flake-shell structures can be formed [28]. The designed silica nanosheets with wide-mounted compartments can disperse Pt nanoparticles and prevent their sintering at high temperature due to the long distance between their particles [29].

For the synthesis of hierarchical self-assembled SAPO-34, the quaternary ammonium organosilane (3-(trimethoxysilyl)propyl)octadecyldimethylammonium chloride (TPOAC) and diethylamine (DEA) were used as the mesopore and the microporous template, respectively. The increase of the TPOAC/tetraethyl orthosilicate (TEOS) ratio affects the crystallization process of SAPO-34, resulting in a change of morphologies, compositions and acidity. ^{13}C and ^{29}Si nuclear magnetic resonance (NMR) results reveal that the TPOAC is a mesoporous template in the SAPO-34 structure [30]. The further approach to obtain hierarchical zeolite nanosheets is the use of TPOAC and TEAOH as templates. The hierarchical assembled SAPO-34 was obtained with sheet-like morphology, attributing to the capping effect of the TPOAC organosilane surfactant. The growth of nanocrystals was suppressed to form sheet-like particles followed by the aggregation of them [31].

Moreover, the synthesis of other zeolite nanosheets or nanolayers such as faujasite (FAU), ferrierite (FER) and Zeolite Socony Mobil - twelve (MTW) zeolite frameworks has been demonstrated [32–37]. TPOAC is one of the most promising mesopore-forming agents, which is widely used in zeolite synthesis. For example, recently FAU zeolite nanosheets were successfully prepared by using an organosilane-surfactant, and TPOAC, as a structure-directing agent. The morphologies and textural properties can be varied by the surfactant content and the crystallization temperature [33,34]. Interestingly, the corn cob ash can also be used as the silica source instead of a commercial sodium silicate to synthesize FAU zeolite nanosheets [35]. In addition, hierarchical FER nanosheets can be obtained by optimizing the suitable amount of TPOAC as the SDA, and they exhibit a higher hierarchy factor (HF value of 0.11) compared with that of conventional FER (HF value of 0.03) [36]. Furthermore, in the synthesis of hierarchical MTW, the ZSM-12 nanolayers were prepared using TPOAC as the secondary SDA. It was found that the amount of TPOAC and the crystallization time are important parameters for the nanolayer formation [37].

2.2. Synthesis of Hierarchical Assembly of Zeolite Nanoparticles

Another approach to obtain hierarchical zeolites is to synthesize the hierarchical assembly of zeolite nanoparticles in which the aggregation of microporous crystals leads to obtaining the inter-crystalline/intra-crystalline mesopores. The hierarchical ZSM-5 zeolites were hydrothermally synthesized using dual templates; tetrapropylammonium hydroxide (TPAOH) as the micropore structure-directing agent, and 3-aminopropyltriethoxysilane (APTES) as the mesopore template agent. The APTES linked on the zeolite surface can interrupt the crystal growth, resulting in the formation of intercrystalline mesoporous zeolites. By increasing the amount of APTES, nanocrystal sizes decreased while mesopore volumes increased [38,39]. Recently, a novel dual-templating synthesis using the $C_{16}H_{33}-[N^+-methylpiperidine]$ ($C_{16}MP$), mono-quaternary ammonium surfactant as mesopore-forming agent, together with a typical structure-directing agent to control the ZSM-5 structure, has been achieved. $C_{16}MP$, which is a cheap surfactant, can be obtained via a single-step synthesis by the alkylation of

n-methylpiperidine. Furthermore, the hierarchical ZSM-5 zeolite can be synthesized using non-charged SDA including diethylamine, *n*-propylamine, 1,4-diaminobutane and 1,6-diaminohexane. The new hierarchical zeolite exhibits high mesoporosity and crystallinity with a low amount of silanol and external Brønsted acid density [40]. TPAOH was also used, together with silica-carbon (SiO₂/C) composites, to synthesize hierarchical zeolites. The carbon amount can control the mesopores by varying the deposition time and the concentration of the carbonaceous gas source [41,42]. The facile, eco-friendly, and cost-effective procedure to synthesize hierarchical ZSM-5 using colloidal silicalite-1 seeds was conceived to reduce the amount of the organic structure-directing agent and to avoid the combustion of the organic templates. The hierarchical porous ZSM-5 aggregates possessed large external surface area and external acidity, mesopore volume, and relatively regular mesopore size distributions. The hierarchical porous ZSM-5 aggregates exhibited excellent performances in the low-density polyethylene (LDPE) catalytic cracking [43]. This procedure is interesting for the synthesis of ZSM-5 nanoparticle assemblies using a lower amount of the template. In addition, zeolite seeds and cetyltrimethylammonium bromide (CTAB) were also used to synthesize hierarchical ZSM-5. The self-assembly and the crystallization step can be controlled by the aid of NaOH and CTAB. The BET surface area, total pore volume and external surface area of hierarchical ZSM-5 samples can be tuned by the amount of CTAB [44,45].

Apart from the hierarchical ZSM-5, the hierarchical Beta zeolite was successfully synthesized with the aid of CTAB via a feasible one-pot and one-step method. The micropore/mesopore ratio can be controlled by the amount of CTAB and the amount of H₂O. This facile synthesis procedure is appropriate for industrial applications [46]. The polymer agent was considered to be used in hierarchical Beta zeolite synthesis [47,48]. The nanoparticle Beta assemblies were obtained using a cationic polymer, polydiallyldimethylammonium chloride (PDDA), as a flocculating agent which performs high mesopore volumes and surface areas [47]. Hierarchical mesoporous Beta microspheres were synthesized using dimethyldiallyl ammonium chloride acrylamide copolymer via one-step procedure. Their hierarchically porous structure facilitates the molecular transport in the catalytic application. This synthesis reveals the facile separation method of filtration instead of centrifugation. Other zeolite frameworks such as ZSM-5, X and Y with hierarchical micro-spherical shapes were also obtained [48]. NaF media in the aerosol-assisted synthesis route was applied to hierarchical Beta zeolite synthesis. The synthesis of the Beta zeolite mainly followed the liquid-phase mechanism. The morphology was changed from spherical nanoaggregates to plate-like crystals when the SiO₂/Al₂O₃ ratio was increased. The hierarchical pores can facilitate the conversion and adsorption of large molecules [49].

For the hierarchical SSZ-13, it can be prepared using trimethyladamantanammonium hydroxide (TMAdaOH) for the CHA framework and a diquatery ammonium surfactant (C₂₂₋₄₋₄Br₂) as the mesoporegen [50]. In addition, various mesoporegens such as C₂₂₋₄₋₄Br₂, C₂₂₋₄Br, C₂₂₋₆₋₆Br₂ and TPOAC were applied together with TMAdaOH to prepare hierarchical SSZ-13 zeolites in a one-step synthesis. The mesopore volume increases with the mesoporegen/SDA ratio as shown in Figure 2. The micropore is used efficiently in the cooperation with the molecular highway mesoporous structures, however the coke formation was also increased at the external surfaces [51].

The ZSM-11 zeolite, one of the Zeolite Socony Mobil-eleven (MEL) structures, which is similar to ZSM-5 zeolite, is also interesting. It is composed of 10-membered ring and 2-dimensional straight channels. The hierarchical ZSM-11 zeolite was successfully synthesized using a small amount of tetrabutylammonium bromide (TBABr) as the SDA. The intergrowth rod-like particles were stacked to form mesoporous structures. The different crystallization conditions can control the morphology and the particle size distribution, which further affects the mesoporous formation [52,53].

Although there are several methods that have been reported for the preparation of various hierarchical zeolite nanosheets and hierarchical assemblies of zeolite nanoparticles, and most of them have been achieved using costly organic structure-directing agent, as a further challenge it would be more interesting to focus on using cheap and commercially available chemicals. In addition, the further

study of the formation mechanism and the controllable decoration of active sites, such as the nature, location, and distribution of active sites, would be addressed.

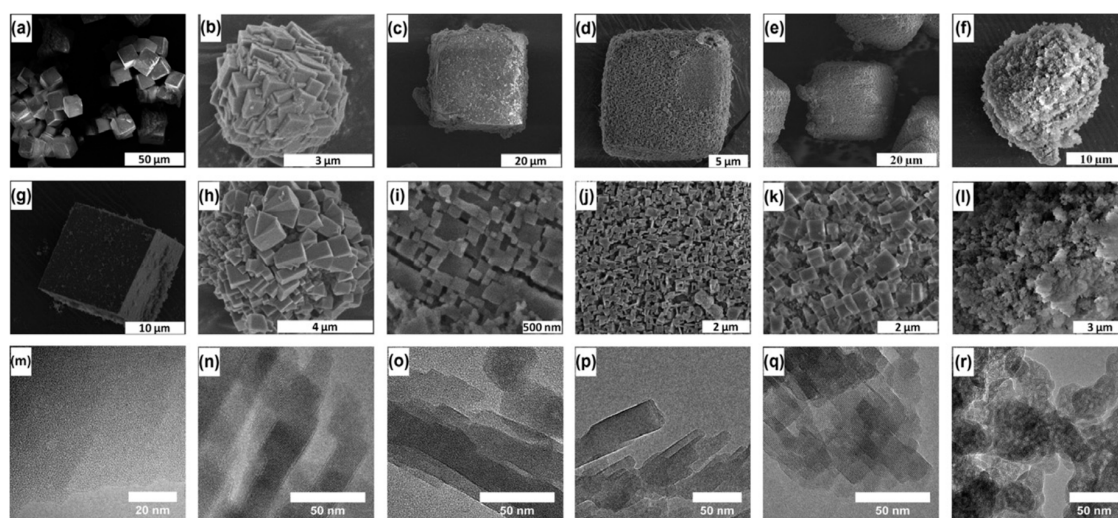


Figure 2. SEM and TEM images: (a,g,m) Conventional SSZ-13; (b,h,n) SSZ-13 (C_{22-44} , 0.06); (c,i,o) SSZ-13 (C_{22-44} , 0.17); (d,j,p) SSZ-13 (C_{22-44} , 0.50); (e,k,q) SSZ-13 (C_{22-44} , 1.50); (f,l,r) SSZ-13 (C_{22-44} , 1). Reprinted with permission from Reference [51]. Copyright (2013), Elsevier.

3. Light Olefin Productions Obtained Using Hierarchical Zeolites

To open up the perspectives of the applications of the above-mentioned hierarchical zeolites, this comprehensive review proposes their benefits for the production of light olefins via methanol/ethanol to light olefins, catalytic cracking and CO_2/CH_4 to light olefins, as shown in the following detail.

3.1. Methanol and Ethanol to Light Olefins

The conversion of methanol/ethanol to light olefins (MTO) is one of the most promising alternative reactions to produce ethylene and propylene for petrochemical building blocks. Typically, CHA zeolites such as SSZ-13 and SAPO-34 have been widely used as catalysts in the MTO reaction. For example, the hierarchical SSZ-13 exhibited a longer catalytic lifetime with respect to the conventional SSZ-13, while the ethylene and propylene selectivity were similar [51]. In a packed bed MTO reactor, the mesoporous SSZ-13 zeolites using 0.17 molar ratio of $C_{22-44}Br_2/TMAdOH$ exhibited an 8.0 h catalytic lifetime, which is longer than that of conventional SSZ-13 (2.8 h) under a similar level of light olefins yield, attributing to the improved accessibility of guest molecules to the micropore space. However, the excess mesopores affected the coke formation at the crystal surface. Thus, a low $C_{22-44}Br_2/TMAdOH$ ratio is suitable for the synthesis of a stable zeolite. These mesoporous SSZ-13 catalysts can be regenerated without losing activity [50]. Furthermore, the hierarchical SSZ-13 catalyst obtained using template-free synthesis exhibits excellent performances in methanol to light olefins, with methanol conversion as high as 100%, high light olefin selectivity at 90%, and with an improved catalyst lifetime compared to a conventional catalyst [54] as shown in Figure 3.

In addition, the catalytic performances of the MTO reaction over the synthesized SAPO-34 were evaluated. The hierarchical nanosheet-assembled SAPO-34 catalyst obtained using dual templates such as TPOAC/TEAOH and TPOAC/DEA exhibits a longer catalytic lifetime and slower coke formation rate and higher light olefin selectivity (81.93%) compared with those of the conventional SAPO-34, which can be attributed to the well retained microporosity, increased mesoporosity and suitable weak acidity [30,31]. The hierarchical SAPO-34 nanoparticles synthesized using carbon nanotubes (CNTs) and diethylamine (DEA) in ultrasound-assisted synthesis were investigated in methanol to olefins. The genetic programming models and the experimental results showed the agreement outputs. The optimal hierarchical SAPO-34 nanoparticles exhibited 94% methanol conversion and

77% light olefins selectivity after 9 h [55]. Interestingly, the SAPO-34 catalysts which were synthesized using morpholine with an inexpensive cationic surfactant (polydiallyldimethylammonium chloride, PDADMAC) showed a 12% enhanced selectivity for ethylene and propylene and a catalytic lifetime more than five times longer than those of conventional catalysts in MTO reactions. The high intracrystalline mesopores increased transport ability and decreased acidity [56]. In addition, the hierarchical nano-sized SAPO-34/18 catalysts using SAPO-34 seed-assisted synthesis exhibit excellent performances in MTO reaction with significantly improved catalytic lifetimes and higher propylene and butylene selectivities. The larger aluminophosphate-eighteen (AEI) cage of SAPO-18 enhances the diffusion of longer alkenes inside the mesopores of thin-plate particles, facilitating a reduction in coke deposition. [57]. Moreover, the introduction of gold in hierarchical SAPO-34 was studied. The Au/SAPO-34 catalyst exhibits a significant improvement of the acidic properties and coke deposition rate of the samples. The synergistic effect of generated mesopores and Au affects the excellent catalytic performance, with a 97% light olefins selectivity and a 331-min lifetime [58].

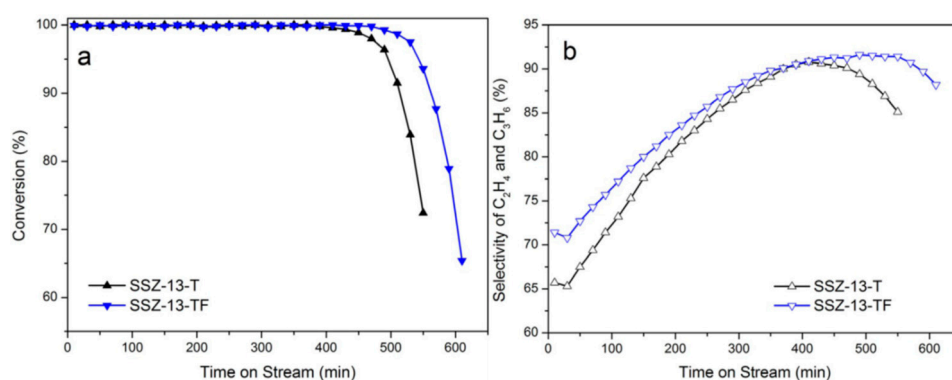


Figure 3. (a) Methanol conversion and (b) selectivity to light olefins as a function of time on stream over SSZ-13 samples ($T = 450\text{ }^{\circ}\text{C}$, $\text{WHSV} = 3\text{ h}^{-1}$). Reproduced with permission from Reference [54]. Copyright 2018, John Wiley & Sons.

In methanol to propylene (MTP), the hierarchical MFI nanosheets were varied with different sheet thicknesses and thinner MFI nanosheets (2.5 nm) exhibited the improved catalytic conversion and catalytic lifetime [59]. The mesopore can improve the diffusion of large molecules and prevent coke formation. Their appropriate acid densities, which have a Si/Al₂ ratio and a B/L ratio around 300–500 and 3.5, respectively, showed the best catalytic performance for propylene production with low further side reactions. In addition, the hierarchical ZSM-5 assemblies obtained using *n*-hexyltrimethylammonium (HTAB) as a mesopore SDA exhibited higher performance in MTP. The hierarchical ZSM-5 catalyst showed higher propylene (40.1%), higher butylene (22.9%) selectivities, and had a significantly longer catalytic lifetime (22 h) compared to the commercial ZSM-5 zeolite. This may refer to the mesoporosity, which increases the external surface and reduces diffusion path lengths, resulting in the utilization of acid sites and preventing further reactions and coke formation [60]. Moreover, the seed-fused ZSM-5 nanosheet (CNS) was synthesized by introducing 5 wt. % seed in the synthetic precursor. When increasing the amount of seed to 30 wt. %, the CNS catalyst improved the catalytic lifetime from 168 to 226 h for methanol to propylene. The boron zeolite nanosheet, B-CNS-5, also exhibited a high catalytic lifetime (302 h) and methanol conversion, because of the lower acidity from B addition, which suppressed coke formation [26].

The hierarchical ZSM-11 zeolites were also used as the catalysts for MTP. The pure silica (Si-ZSM-11) showed a high performance in MTP and exhibited a higher propylene/ethylene ratio and lower deactivation rate compared with those of H-ZSM-11 with a similar Si/Al of 26. The H-bond in the silanol group of Si-ZSM-11 affects the production of propene and butene [61]. The introduction of phosphorus into the hierarchical ZSM-11 framework was studied in the MTP reaction. The hierarchical ZSM-11 zeolite with a P/Al ratio of 0.2 enhanced the high yield of propene (20.35 wt. %) and catalytic

stability, attributing to the optimum amount of P, which could reduce strong Brønsted acid sites while it can maintain the ZSM-11 structure, suppressing the hydrogen transfer and cyclization reactions. The higher P amount ($P/Al > 0.2$) affects lower catalytic activity because the crystallinity, acidity, pore volume and surface area were decreased [62].

Furthermore, the hierarchical zeolites were also investigated in ethanol dehydration to ethylene. At mild temperatures of 300–350 °C, the hierarchical ZSM-5 nanosheets exhibit high ethanol conversion around 90%, high ethylene selectivity around 85% and high stability. From the computational results, the ethylene might occur using the Brønsted acid sites at the external surfaces of MFI, whereas diethyl ether is the major reaction using the internal Brønsted acid sites [63].

In addition, the hierarchical core-shell composites, which have medium acidity at the surface, can enhance catalytic performance and catalyst stability. Compared with SAPO-34, the SAPO-34@ZSM-5 and SAPO-34@silicalite-1 composites exhibit higher propylene and ethylene yield, respectively. With respect to ZSM-5, the ethylene and propylene selectivity on SAPO-34@ZSM-5 and silicalite-1@ZSM-5 could be improved from 74% to 80% and 99%, respectively [64].

3.2. Catalytic Cracking and Dehydrogenation of Alkanes

Besides, the catalytic cracking of alkanes to light olefins has been studied on hierarchical zeolite nanosheets and nanoparticle assemblies. The hierarchical ZSM-5 having mesopores improves the catalytic stability due to decreasing the diffusion path-length, suppressing the further reactions and reducing the coke formation in the catalytic cracking of *n*-hexane [42,65]. The hierarchical ZSM-5 catalysts obtained using a carbon template were investigated in the C₅ raffinate cracking. When increasing the amount of carbon template, mesopore volume increased, resulting in higher C₅ raffinate conversion and light olefins yield, with similar ethylene and propylene selectivity [66]. In the catalytic cracking of *n*-heptane, ZSM-5 nanosheets with highly exposed (010) planes exhibited outstanding performance of high conversion and stability, attributed to the hierarchical porosity of the unique planes. The accessibility of microporous acid sites and facile mass transfer of bulky molecules were enhanced [67]. Some studies reveal that the mesopore can increase the diffusion rate of light olefins inside the zeolite network. This reason makes the ethylene and propylene transfer out of micropores quickly, and then the consecutive reaction can be suppressed [39]. Due to this reason, in the *n*-heptane cracking, the hierarchical ZSM-5 zeolite nanocrystals exhibited high light olefins selectivity with a low coking amount. The mesopore provides short diffusion path lengths and lower diffusion limitation, which enhance light olefins yield and prevent the coke deposition [26]. Interestingly, the pillared HZSM-5 nanosheets were prepared by following two approaches: (i) using a dual template (denoted as DZN-2 catalyst); (ii) Si precursor intercalation in which TEOS penetrated into the surfactant region (denoted as PZN-2 catalyst). In the catalytic cracking of *n*-decane at 500 °C, DZN-2 performed the highest selectivity of light olefins at 37.8%, and *n*-decane conversion around 92%, compared with those of PZN-2 and the typical zeolite nanosheet (ZN-2) as shown in Figure 4. Moreover, DZN-2 showed high catalytic stability and a low deactivation rate because the pillar structure facilitated product diffusion and suppressed the consecutive reactions [68].

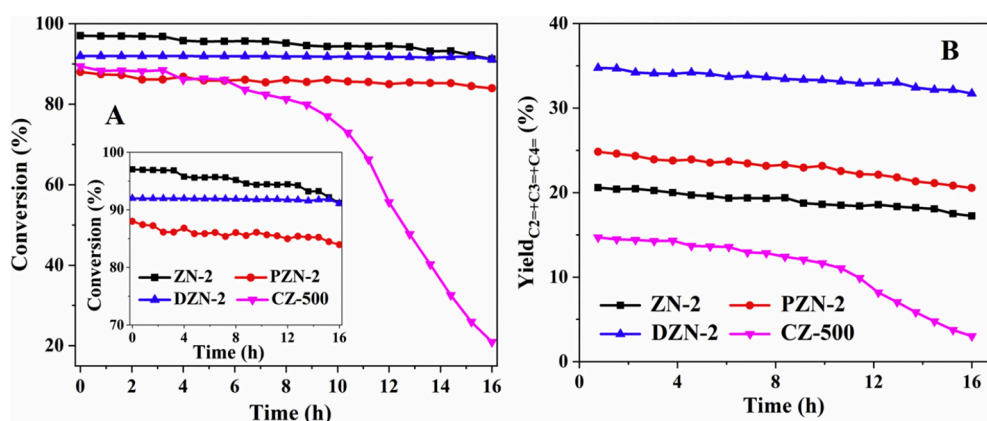


Figure 4. (A) *n*-decane conversion; (B) yields of light olefins as a function of reaction time on different catalysts ($T = 500\text{ }^{\circ}\text{C}$, $\text{WHSV} = 8.76\text{ h}^{-1}$). Reprinted with permission from Reference [68]. Copyright (2019), Elsevier.

In addition, the combination of hierarchical zeolites and tartaric acid treatment can provide a highly efficient catalyst. In *n*-heptane catalytic cracking, the hierarchical ZSM-5 exhibited higher selectivity to light olefins and low coke deposition with respect to normal hierarchical zeolites. After tartaric acid treatment, the external acid sites are selectively removed. The ethylene and propylene selectivity can be improved due to preventing the consecutive reactions of light olefin products [69]. The effect of metals loaded by MFI nanosheet zeolites (MFI (M), $M = \text{Al, Ga, and Fe}$) on the catalytic performance of *n*-dodecane cracking was studied. The MFI nanosheet zeolites exhibited higher light alkenes and lower deactivation rates than those of the ZSM-5 zeolite. The Ga substitution affected the decrease of acid strength, which had a positive effect on the catalytic cracking of *n*-dodecane and may enhance light olefins yield [70]. Moreover, the catalytic cracking of light naphtha was investigated. The hierarchical ZSM-5 zeolite prepared using a template of 15 wt. % carbon nanotubes exhibited the highest olefin yield (54 wt. %) and catalytic lifetime compared to the other synthesized catalysts. The hierarchical structure with appropriate acidity facilitated diffusion of reactants and products [71]. In the other catalytic cracking reactions, the catalytic cracking of triglycerides was studied, for example. The hierarchical ZSM-5 exhibited a high conversion of 14%, with high gasoline and light olefin yields of 10%, and 30%, respectively, ascribed to increased accessibility of maintaining microporous acid sites and mass transfer of molecules in the mesoporous structures [72].

Furthermore, the introduction of metals such as Ga and Pt over hierarchical zeolites was also studied in propane dehydrogenation to propylene. The hierarchical Ga-MFI catalysts have a higher Lewis acid site with respect to conventional Ga-MFI. For this reason, the hierarchical Ga-MFI catalysts exhibit improved propylene selectivity from 35% to 80% at $600\text{ }^{\circ}\text{C}$. The higher performance relates to a lower propylene adsorption and the Brønsted and Lewis acid sites distribution around the mesopores [73]. In addition, the Pt silicalite-1 nanosheets exhibit high propylene selectivity around 95% because they can prohibit the side reaction and reduce the diffusion limitation. The presence of ultra-small Pt particles dispersed on defect surfaces of silicalite-1 nanosheets was confirmed [74].

3.3. CO_2/CH_4 to Light Olefins

Due to the importance of ethylene, propylene and butylene, the direct production of light olefins from CO_2 and CH_4 is also very interesting. Presently, there are some studies that report on the conversion of CO_2 to light olefins on hierarchical acid zeolites incorporated with metal oxides. For example, In_2O_3 is widely used as CO_2 in a hydrogenation catalyst [75]. To combine metal oxides together with acid catalysts, the zeolites were prepared by integrating with various metal oxides such as indium, zirconium, and zinc oxide. In CO_2 hydrogenation, the $\text{In}_2\text{O}_3/\text{ZrO}_2$ and SAPO-34, which are methanol and light olefins synthesis catalysts, respectively, were investigated [76,77]. At the typical

condition, $\text{In}_2\text{O}_3/\text{ZrO}_2$ and SAPO-34 with the ratio of 1:1 show a selectivity of light olefins of up to 80–90%, with CO_2 conversion around 20% [76]. To compare the catalytic activity among catalysts prepared by different methods, the In-Zr oxide and SAPO-34 samples were prepared by dual-bed, granule-mixing and mortar-mixing methods. The In-Zr/SAPO-34 using granule-mixing exhibits CO_2 conversion up to 35%, high light olefin selectivity around 80%, and low methane selectivity only 4% [77]. In addition, Zn oxide was also incorporated in SAPO-34. The physical mixture of ZnO-ZrO_2 and Zn-SAPO-34, of which the small ZnO-ZrO_2 particles can disperse on the surface of Zn-SAPO-34, illustrates a light olefins selectivity up to 80–90% [78]. Moreover, hierarchical bifunctional catalysts, prepared by physical mixing between In_2O_3 and ZnZrO_x oxides supported on SAPO-34 zeolites with different crystal sizes (0.4–1.5 mm) were investigated for CO_2 conversion. It was found that the acid-treated SAPO-34 catalysts generated a suitable Brønsted acid and hierarchical pores, facilitating the intermediates and products transportation. Eventually, they exhibited a very high $\text{C}_2^=-\text{C}_4^=-$ selectivity of 85%, with only 1% CH_4 selectivity at the CO_2 conversion level of 17% [79] as shown in Figure 5.

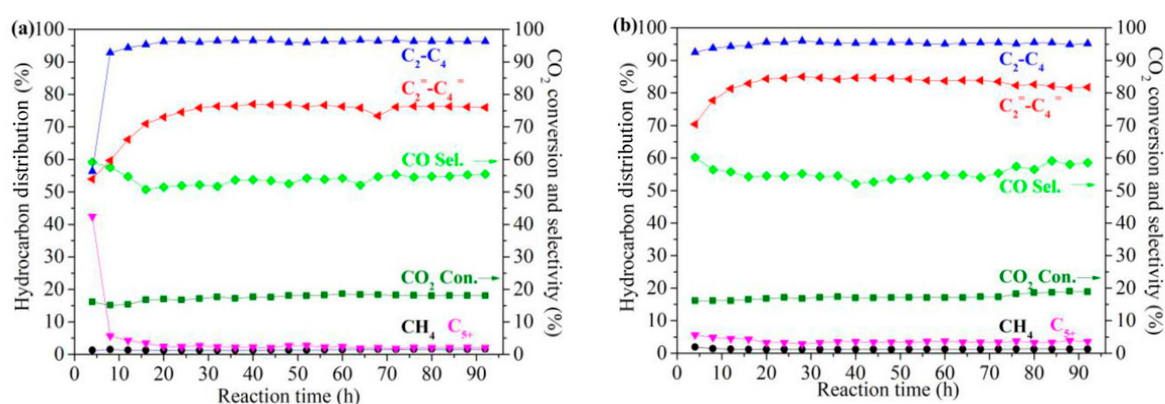


Figure 5. Stability tests of bifunctional catalysts. (a) $\text{In}_2\text{O}_3\text{-ZnZrO}_x/\text{SAPO-34-C}$; (b) $\text{In}_2\text{O}_3\text{-ZnZrO}_x/\text{SAPO-34-H-a}$. Catalysts with oxide/zeolite mass ratio = 0.5. Reaction conditions: 380 °C, 3.0 MPa, 9000 mL $\text{g}_{\text{cat}}^{-1} \text{h}^{-1}$, $\text{H}_2/\text{CO}_2/\text{N}_2=73:24:3$. Reproduced with permission from Reference [79]. Copyright 2019, John Wiley & Sons.

Recently, the CH_4 conversion to light olefins has also been widely studied. For example, the one-step methane transformation to light olefins at mild temperature was successfully investigated using H-SAPO-34 in the presence of halide such as bromine or chlorine. Interestingly, at the optimized condition (83 s contact time and 365 °C), methane was converted to methyl bromide and subsequently changed partially to hydrocarbons with ethylene and propylene selectivities of 15.0% and 8.3%, respectively [80]. To evaluate the effect of mesoporous structure, hierarchical ZSM-5 catalysts were preliminarily tested in chloromethane conversion to light olefins (CMTO). The two hierarchical porous ZSM-5 (HP-ZSM-5) catalysts were prepared using an organosilane-assisted template and a triethoxy-vinylsilane as the growth inhibitor [81,82]. Interestingly, compared with a conventional catalyst, the HP-ZSM-5 obtained by using organosilane performed an increased light olefins selectivity from 44.1% to 68.1%, and the high conversion of chloromethane of 98% even after 72 h of reaction time, and this behavior is four times longer than that of a conventional one [81]. In addition, the HP-ZSM-5 obtained by using a growth inhibitor shows the high performance of CMTO in which light olefins selectivity is 69.3% and the high catalytic stability is still observed even after 115 h of reaction time. This work illustrates the perspectives that mesopores can increase molecular transportation and decrease strong acidity, eventually suppressing the consecutive reactions [82].

4. Conclusions and Future Perspectives

This comprehensive review demonstrates the recent progress in the development of hierarchical zeolite nanosheets and nanoparticle assemblies with various zeolite frameworks including MFI,

MEL, CHA, BEA, FAU, FER and MTW. Mostly, they have been obtained using various procedures ranging from single-template synthesis, to multiple-template synthesis and seed-assisted synthesis. The diquaternary ammonium structures have been widely used as bifunctional structure-directing agents for controlling both mesoporous and microporous structures, eventually resulting in improved mesoporosity while the micropore structure in the zeolite framework is still maintained. However, the molar ratio of template should be adjusted properly, because the excess mesoporosity can affect coke deposition on the zeolite surface.

According to the light olefin productions, most hierarchical catalysts exhibit high conversion, high light olefins selectivity and long lifetimes for many light olefin production processes, ranging from MTO, to catalytic cracking and CO₂/CH₄ conversion, due to an increase in external surface areas, reducing the diffusion path-length, and eventually resulting in the improved accessibility of guest molecules into acid sites and lower coke formation. Moreover, the introduction of other heteroatoms such as boron and phosphorous into the zeolite framework can suppress further reaction due to the modification of acidity of zeolite surfaces.

Until now, although there are many developed hierarchical zeolite nanosheets and hierarchical assemblies of zeolite nanoparticles, most of them have been achieved using costly organic structure-directing agent. It would be highly interesting for further perspectives to focus on using cheap and commercially available chemicals and to gain insights into the formation mechanism. The nature, location, and distribution of active sites in hierarchical structures would be addressed. In addition, the application of such designed materials is still in the early stage of development, in particular, with the production of light olefins such as methanol/ethanol to light olefins, catalytic cracking and CO₂/CH₄ conversion. The primary challenge in their application in light olefins production is the lack of understanding in deep details according to catalytic mechanism, coke formation and locations, the effect of hierarchical structure and Al distribution on the light olefin product selectivity, the reusability and stability of hierarchical zeolites, as well as the diffusion and kinetics aspects. In addition to these challenges, the feasibility of using hierarchical zeolites on a commercialization scale is still missing. In the perspective of conclusion, despite the fact that the use of hierarchical zeolite nanosheets and nanoparticle assemblies has not yet been widely used on a real commercial scale, it is promising for the future that such designed materials would demonstrate the possibility of being promising catalysts in the production of light olefins.

Author Contributions: Conceptualization, P.D. and C.W.; writing—original draft preparation, P.D.; writing—review and editing, P.D. and C.W.; supervision, C.W. All authors have read and agreed to the published version of the manuscript.

Funding: This research was funded by the Vidyasirimedhi Institute of Science and Technology, TTSF research project supported by Thailand Toray Science Foundation, Thailand Research Fund (MRG6180099), and the Office of Higher Education Commission. In addition, this work has been partially supported by the National Nanotechnology Center (NANOTEC), NSTDA, Ministry of Science and Technology, Thailand, through its program of Research Network NANOTEC.

Conflicts of Interest: The authors declare no conflict of interest.

References

1. Corma, A.; Melo, F.V.; Sauvanaud, L.; Ortega, F. Light cracked naphtha processing: Controlling chemistry for maximum propylene production. *Catal. Today* **2005**, *107–108*, 699–706. [[CrossRef](#)]
2. Wei, Y.; Liu, Z.; Wang, G.; Qi, Y.; Xu, L.; Xie, P.; He, Y. Production of light olefins and aromatic hydrocarbons through catalytic cracking of naphtha at lowered temperature. In *Studies in Surface Science and Catalysis*; Čejka, J., Žilková, N., Nachtigall, P., Eds.; Elsevier: Amsterdam, The Netherlands, 2005; Volume 158, pp. 1223–1230.
3. Sadrameli, S.M. Thermal/catalytic cracking of liquid hydrocarbons for the production of olefins: A state-of-the-art review II: Catalytic cracking review. *Fuel* **2016**, *173*, 285–297. [[CrossRef](#)]
4. Corma, A. From microporous to mesoporous molecular sieve materials and their use in catalysis. *Chem. Rev.* **1997**, *97*, 2373–2420. [[CrossRef](#)] [[PubMed](#)]

5. Hillhouse, H.W.; Okubo, T.; van Egmond, J.W.; Tsapatsis, M. Preparation of supported mesoporous silica layers in a continuous flow cell. *Chem. Mater.* **1997**, *9*, 1505–1507. [[CrossRef](#)]
6. Hirai, T.; Okubo, H.; Komasaawa, I. Size-selective incorporation of CdS nanoparticles into mesoporous silica. *J. Phys. Chem. B* **1999**, *103*, 4228–4230. [[CrossRef](#)]
7. Christensen, C.H.; Johannsen, K.; Schmidt, I.; Christensen, C.H. Catalytic benzene alkylation over mesoporous zeolite single crystals: Improving activity and selectivity with a new family of porous materials. *J. Am. Chem. Soc.* **2003**, *125*, 13370–13371. [[CrossRef](#)]
8. Fan, W.; Snyder, M.A.; Kumar, S.; Lee, P.-S.; Yoo, W.C.; McCormick, A.V.; Lee Penn, R.; Stein, A.; Tsapatsis, M. Hierarchical nanofabrication of microporous crystals with ordered mesoporosity. *Nat. Mater.* **2008**, *7*, 984–991. [[CrossRef](#)]
9. Pérez-Ramírez, J.; Christensen, C.H.; Egeblad, K.; Christensen, C.H.; Groen, J.C. Hierarchical zeolites: Enhanced utilisation of microporous crystals in catalysis by advances in materials design. *Chem. Soc. Rev.* **2008**, *37*, 2530–2542. [[CrossRef](#)]
10. Choi, M.; Na, K.; Kim, J.; Sakamoto, Y.; Terasaki, O.; Ryoo, R. Stable single-unit-cell nanosheets of zeolite MFI as active and long-lived catalysts. *Nature* **2009**, *461*, 246–249. [[CrossRef](#)]
11. Na, K.; Choi, M.; Park, W.; Sakamoto, Y.; Terasaki, O.; Ryoo, R. Pillared MFI zeolite nanosheets of a single-unit-cell thickness. *J. Am. Chem. Soc.* **2010**, *132*, 4169–4177. [[CrossRef](#)]
12. Na, K.; Park, W.; Seo, Y.; Ryoo, R. Disordered assembly of MFI zeolite nanosheets with a large volume of intersheet mesopores. *Chem. Mater.* **2011**, *23*, 1273–1279. [[CrossRef](#)]
13. Emdadi, L.; Wu, Y.; Zhu, G.; Chang, C.-C.; Fan, W.; Pham, T.; Lobo, R.F.; Liu, D. Dual template synthesis of meso- and microporous MFI zeolite nanosheet assemblies with tailored activity in catalytic reactions. *Chem. Mater.* **2014**, *26*, 1345–1355. [[CrossRef](#)]
14. Tian, Y.; Liu, H.; Wang, L.; Zhang, X.; Liu, G. Controllable fabrication and catalytic performance of nanosheet HZSM-5 films by vertical secondary growth. *AIChE J.* **2018**, *64*, 1923–1927. [[CrossRef](#)]
15. Simone, N.; Carvalho, W.A.; Mandelli, D.; Ryoo, R. Nanostructured MFI-type zeolites as catalysts in glycerol etherification with tert-butyl alcohol. *J. Mol. Catal. A Chem.* **2016**, *422*, 115–121. [[CrossRef](#)]
16. Park, W.; Yu, D.; Na, K.; Jelfs, K.E.; Slater, B.; Sakamoto, Y.; Ryoo, R. Hierarchically structure-directing effect of multi-ammonium surfactants for the generation of MFI zeolite nanosheets. *Chem. Mater.* **2011**, *23*, 5131–5137. [[CrossRef](#)]
17. Choi, M.; Cho, H.S.; Srivastava, R.; Venkatesan, C.; Choi, D.-H.; Ryoo, R. Amphiphilic organosilane-directed synthesis of crystalline zeolite with tunable mesoporosity. *Nat. Mater.* **2006**, *5*, 718–723. [[CrossRef](#)]
18. Rani, P.; Srivastava, R.; Satpati, B. One-step dual template mediated synthesis of nanocrystalline zeolites of different framework structures. *Cryst. Growth Des.* **2016**, *16*, 3323–3333. [[CrossRef](#)]
19. Barakov, R.; Shcherban, N.; Yaremov, P.; Bezverkhyi, I.; Baranchikov, A.; Trachevskii, V.; Tsyryna, V.; Ilyin, V. Synthesis of micro-mesoporous aluminosilicates on the basis of ZSM-5 zeolite using dual-functional templates at presence of micellar and molecular templates. *Microporous Mesoporous Mater.* **2017**, *237*, 90–107. [[CrossRef](#)]
20. Xu, D.; Ma, Y.; Jing, Z.; Han, L.; Singh, B.; Feng, J.; Shen, X.; Cao, F.; Oleynikov, P.; Sun, H.; et al. π - π interaction of aromatic groups in amphiphilic molecules directing for single-crystalline mesostructured zeolite nanosheets. *Nat. Commun.* **2014**, *5*, 4262. [[CrossRef](#)]
21. Liu, B.; Duan, Q.; Li, C.; Zhu, Z.; Xi, H.; Qian, Y. Template synthesis of the hierarchically structured MFI zeolite with nanosheet frameworks and tailored structure. *New J. Chem.* **2014**, *38*, 4380–4387. [[CrossRef](#)]
22. Liu, B.; Chen, Z.; Huang, J.; Chen, H.; Fang, Y. Direct synthesis of hierarchically structured MFI zeolite nanosheet assemblies with tailored activity in benzylation reaction. *Microporous Mesoporous Mater.* **2019**, *273*, 235–242. [[CrossRef](#)]
23. Zhang, X.; Liu, D.; Xu, D.; Asahina, S.; Cychosz, K.A.; Agrawal, K.V.; Al Wahedi, Y.; Bhan, A.; Al Hashimi, S.; Terasaki, O.; et al. Synthesis of self-pillared zeolite nanosheets by repetitive branching. *Science* **2012**, *336*, 1684–1687. [[CrossRef](#)] [[PubMed](#)]
24. Wannapakdee, W.; Wattanakit, C.; Paluka, V.; Yutthalekha, T.; Limtrakul, J. One-pot synthesis of novel hierarchical bifunctional Ga/HZSM-5 nanosheets for propane aromatization. *RSC Adv.* **2016**, *6*, 2875–2881. [[CrossRef](#)]
25. Wannapakdee, W.; Suttipat, D.; Dugkhuntod, P.; Yutthalekha, T.; Thivasasith, A.; Kidkhunthod, P.; Nokbin, S.; Pengpanich, S.; Limtrakul, J.; Wattanakit, C. Aromatization of C₅ hydrocarbons over Ga-modified hierarchical HZSM-5 nanosheets. *Fuel* **2019**, *236*, 1243–1253. [[CrossRef](#)]

26. Shang, Y.; Wang, W.; Zhai, Y.; Song, Y.; Zhao, X.; Ma, T.; Wei, J.; Gong, Y. Seed-fused ZSM-5 nanosheet as a superior MTP catalyst: Synergy of micro/mesopore and inter/external acidity. *Microporous Mesoporous Mater.* **2019**, *276*, 173–182. [[CrossRef](#)]
27. Camarota, B.; Mann, S.; Onida, B.; Garrone, E. Hierarchical self-assembly in molecularly ordered phenylene-bridged mesoporous organosilica nanofilaments. *ChemPhysChem* **2007**, *8*, 2363–2366. [[CrossRef](#)]
28. Ji, Q.; Guo, C.; Yu, X.; Ochs, C.J.; Hill, J.P.; Caruso, F.; Nakazawa, H.; Ariga, K. Flake-shell capsules: Adjustable inorganic structures. *Small* **2012**, *8*, 2345–2349. [[CrossRef](#)] [[PubMed](#)]
29. Liu, J.; Ji, Q.; Imai, T.; Ariga, K.; Abe, H. Sintering-resistant nanoparticles in wide-mouthed compartments for sustained catalytic performance. *Sci. Rep.* **2017**, *7*, 41773. [[CrossRef](#)]
30. Wang, C.; Yang, M.; Tian, P.; Xu, S.; Yang, Y.; Wang, D.; Yuan, Y.; Liu, Z. Dual template-directed synthesis of SAPO-34 nanosheet assemblies with improved stability in the methanol to olefins reaction. *J. Mater. Chem. A* **2015**, *3*, 5608–5616. [[CrossRef](#)]
31. Chen, H.; Wang, M.; Yang, M.; Shang, W.; Yang, C.; Liu, B.; Hao, Q.; Zhang, J.; Ma, X. Organosilane surfactant-directed synthesis of nanosheet-assembled SAPO-34 zeolites with improved MTO catalytic performance. *J. Mater. Sci.* **2019**, *54*, 8202–8215. [[CrossRef](#)]
32. Inayat, A.; Knoke, I.; Spiecker, E.; Schwieger, W. Assemblies of mesoporous FAU-type zeolite nanosheets. *Angew. Chem. Int. Ed. Engl.* **2012**, *51*, 1962–1965. [[CrossRef](#)]
33. Yuthalekha, T.; Wattanakit, C.; Warakulwit, C.; Wannapakdee, W.; Rodponthukwaji, K.; Witoon, T.; Limtrakul, J. Hierarchical FAU-type zeolite nanosheets as green and sustainable catalysts for benzylation of toluene. *J. Clean. Prod.* **2017**, *142*, 1244–1251. [[CrossRef](#)]
34. Yuthalekha, T.; Suttipat, D.; Salakhum, S.; Thivasasith, A.; Nokbin, S.; Limtrakul, J.; Wattanakit, C. Aldol condensation of biomass-derived platform molecules over amine-grafted hierarchical FAU-type zeolite nanosheets (Zeolean) featuring basic sites. *Chem. Commun.* **2017**, *53*, 12185–12188. [[CrossRef](#)] [[PubMed](#)]
35. Salakhum, S.; Yuthalekha, T.; Chareonpanich, M.; Limtrakul, J.; Wattanakit, C. Synthesis of hierarchical faujasite nanosheets from corn cob ash-derived nanosilica as efficient catalysts for hydrogenation of lignin-derived alkylphenols. *Microporous Mesoporous Mater.* **2018**, *258*, 141–150. [[CrossRef](#)]
36. Wuamprakhon, P.; Wattanakit, C.; Warakulwit, C.; Yuthalekha, T.; Wannapakdee, W.; Ittisanronnachai, S.; Limtrakul, J. Direct synthesis of hierarchical ferrierite nanosheet assemblies via an organosilane template approach and determination of their catalytic activity. *Microporous Mesoporous Mater.* **2016**, *219*, 1–9. [[CrossRef](#)]
37. Dugkhuntod, P.; Imyen, T.; Wannapakdee, W.; Yuthalekha, T.; Salakhum, S.; Wattanakit, C. Synthesis of hierarchical ZSM-12 nanolayers for levulinic acid esterification with ethanol to ethyl levulinate. *RSC Adv.* **2019**, *9*, 18087–18097. [[CrossRef](#)]
38. Xu, S.; Zhang, X.; Cheng, D.-G.; Chen, F.; Ren, X. Effect of hierarchical ZSM-5 zeolite crystal size on diffusion and catalytic performance of *n*-heptane cracking. *Front. Chem. Sci. Eng.* **2018**, *12*, 780–789. [[CrossRef](#)]
39. Zhang, X.; Cheng, D.-G.; Chen, F.; Zhan, X. *n*-Heptane catalytic cracking on hierarchical ZSM-5 zeolite: The effect of mesopores. *Chem. Eng. Sci.* **2017**, *168*, 352–359. [[CrossRef](#)]
40. Meng, L.; Zhu, X.; Wannapakdee, W.; Pestman, R.; Goesten, M.G.; Gao, L.; van Hoof, A.J.F.; Hensen, E.J.M. A dual-templating synthesis strategy to hierarchical ZSM-5 zeolites as efficient catalysts for the methanol-to-hydrocarbons reaction. *J. Catal.* **2018**, *361*, 135–142. [[CrossRef](#)]
41. Wattanakit, C.; Warakulwit, C.; Pantu, P.; Sunpetch, B.; Charoenpanich, M.; Limtrakul, J. The versatile synthesis method for hierarchical micro- and mesoporous zeolite: An embedded nanocarbon cluster approach. *Can. J. Chem. Eng.* **2012**, *90*, 873–880. [[CrossRef](#)]
42. Imyen, T.; Wannapakdee, W.; Limtrakul, J.; Wattanakit, C. Role of hierarchical micro-mesoporous structure of ZSM-5 derived from an embedded nanocarbon cluster synthesis approach in isomerization of alkenes, catalytic cracking and hydrocracking of alkanes. *Fuel* **2019**, *254*, 115593. [[CrossRef](#)]
43. Xue, T.; Li, S.; Wu, H.; Wu, P.; He, M. Eco-friendly and cost-effective synthesis of ZSM-5 aggregates with hierarchical porosity. *Ind. Eng. Chem. Res.* **2017**, *56*, 13535–13542. [[CrossRef](#)]
44. Jin, L.; Liu, S.; Xie, T.; Wang, Y.; Guo, X.; Hu, H. Synthesis of hierarchical ZSM-5 by cetyltrimethylammonium bromide assisted self-assembly of zeolite seeds and its catalytic performances. *React. Kinet. Mech. Cat.* **2014**, *113*, 575–584. [[CrossRef](#)]

45. Wannapakdee, W.; Meng, L.; van Hoof, A.J.F.; Bolshakov, A.; Wattanakit, C.; Hensen, E.J.M. The important role of rubidium hydroxide in the synthesis of hierarchical ZSM-5 zeolite using cetyltrimethylammonium as structure-directing agent. *Eur. J. Inorg. Chem.* **2019**, *2019*, 2493–2497. [[CrossRef](#)]
46. Zhang, W.; Ming, W.; Hu, S.; Qin, B.; Ma, J.; Li, R. A feasible one-step synthesis of hierarchical zeolite Beta with uniform nanocrystals via CTAB. *Materials* **2018**, *11*, 651. [[CrossRef](#)]
47. Möller, K.; Yilmaz, B.; Müller, U.; Bein, T. Hierarchical zeolite Beta via nanoparticle assembly with a cationic polymer. *Chem. Mater.* **2011**, *23*, 4301–4310. [[CrossRef](#)]
48. Yin, C.; Tian, D.; Xu, M.; Wei, Y.; Bao, X.; Chen, Y.; Wang, F. One-step synthesis of hierarchical mesoporous zeolite Beta microspheres from assembly of nanocrystals. *J. Colloid Interface Sci.* **2013**, *397*, 108–113. [[CrossRef](#)]
49. Xiong, G.; Feng, M.; Liu, J.; Meng, Q.; Liu, L.; Guo, H. The synthesis of hierarchical high-silica beta zeolites in NaF media. *RSC Adv.* **2019**, *9*, 3653–3660. [[CrossRef](#)]
50. Wu, L.; Degirmenci, V.; Magusin, P.C.M.M.; Szyja, B.M.; Hensen, E.J.M. Dual template synthesis of a highly mesoporous SSZ-13 zeolite with improved stability in the methanol-to-olefins reaction. *Chem. Commun.* **2012**, *48*, 9492–9494. [[CrossRef](#)]
51. Wu, L.; Degirmenci, V.; Magusin, P.C.M.M.; Lousberg, N.J.H.G.M.; Hensen, E.J.M. Mesoporous SSZ-13 zeolite prepared by a dual-template method with improved performance in the methanol-to-olefins reaction. *J. Catal.* **2013**, *298*, 27–40. [[CrossRef](#)]
52. Yu, Q.; Cui, C.; Zhang, Q.; Chen, J.; Li, Y.; Sun, J.; Li, C.; Cui, Q.; Yang, C.; Shan, H. Hierarchical ZSM-11 with intergrowth structures: Synthesis, characterization and catalytic properties. *J. Energy Chem.* **2013**, *22*, 761–768. [[CrossRef](#)]
53. Zhang, L.; Shan, W.; Ke, M.; Song, Z. Synthesis of hierarchical nano-MEL zeolites with controlled sizes using template-free BEA seeds for oligomerization of butene to liquid fuel with high conversion efficiency. *Catal. Commun.* **2019**, *124*, 36–40. [[CrossRef](#)]
54. Bing, L.; Tian, A.; Wang, F.; Yi, K.; Sun, X.; Wang, G. Template-free synthesis of hierarchical SSZ-13 microspheres with high MTO catalytic activity. *Chem. Eur. J.* **2018**, *24*, 7428–7433. [[CrossRef](#)] [[PubMed](#)]
55. Azarhoosh, M.J.; Halladj, R.; Askari, S.; Aghaeinejad-Meybodi, A. Performance analysis of ultrasound-assisted synthesized nano-hierarchical SAPO-34 catalyst in the methanol-to-lights-olefins process via artificial intelligence methods. *Ultrason. Sonochem.* **2019**, *58*, 104646. [[CrossRef](#)] [[PubMed](#)]
56. Guo, G.; Sun, Q.; Wang, N.; Bai, R.; Yu, J. Cost-effective synthesis of hierarchical SAPO-34 zeolites with abundant intracrystalline mesopores and excellent MTO performance. *Chem. Commun.* **2018**, *54*, 3697–3700. [[CrossRef](#)]
57. Chang, N.; Bai, L.; Zhang, Y.; Zeng, G. Fast synthesis of hierarchical CHA/AEI intergrowth zeolite with ammonium salts as mineralizing agent and its application for MTO process. *Chem. Pap.* **2019**, *73*, 221–237. [[CrossRef](#)]
58. Rami, M.D.; Taghizadeh, M.; Akhoundzadeh, H. Synthesis and characterization of nano-sized hierarchical porous AuSAPO-34 catalyst for MTO reaction: Special insight on the influence of TX-100 as a cheap and green surfactant. *Microporous Mesoporous Mater.* **2019**, *285*, 259–270. [[CrossRef](#)]
59. Kim, Y.; Kim, J.-C.; Jo, C.; Kim, T.-W.; Kim, C.-U.; Jeong, S.-Y.; Chae, H.-J. Structural and physicochemical effects of MFI zeolite nanosheets for the selective synthesis of propylene from methanol. *Microporous Mesoporous Mater.* **2016**, *222*, 1–8. [[CrossRef](#)]
60. Li, H.; Wang, Y.; Meng, F.; Gao, F.; Sun, C.; Fan, C.; Wang, X.; Wang, S. Controllable fabrication of single-crystalline, ultrafine and high-silica hierarchical ZSM-5 aggregates via solid-like state conversion. *RSC Adv.* **2017**, *7*, 25605–25620. [[CrossRef](#)]
61. Meng, X.; Yu, Q.; Gao, Y.; Zhang, Q.; Li, C.; Cui, Q. Enhanced propene/ethene selectivity for methanol conversion over pure silica zeolite: Role of hydrogen-bonded silanol groups. *Catal. Commun.* **2015**, *61*, 67–71. [[CrossRef](#)]
62. Huang, H.; Meng, X.; Chen, C.; Zhang, M.; Meng, Z.; Li, C.; Cui, Q. Effect of phosphorus addition on the performance of hierarchical ZSM-11 catalysts in methanol to propene reaction. *Catal. Lett.* **2016**, *146*, 2357–2363. [[CrossRef](#)]
63. Shetsiri, S.; Thivasasith, A.; Saenluang, K.; Wannapakdee, W.; Salakhum, S.; Wetchasat, P.; Nokbin, S.; Limtrakul, J.; Wattanakit, C. Sustainable production of ethylene from bioethanol over hierarchical ZSM-5 nanosheets. *Sustain. Energy Fuels* **2019**, *3*, 115–126. [[CrossRef](#)]

64. Li, X.; Rezaei, F.; Ludlow, D.K.; Rownaghi, A.A. Synthesis of SAPO-34@ZSM-5 and SAPO-34@silicalite-1 core-shell zeolite composites for ethanol dehydration. *Ind. Eng. Chem. Res.* **2018**, *57*, 1446–1453. [[CrossRef](#)]
65. Li, W.; Ma, T.; Zhang, Y.; Gong, Y.; Wu, Z.; Dou, T. Facile control of inter-crystalline porosity in the synthesis of size-controlled mesoporous MFI zeolites via in situ conversion of silica gel into zeolite nanocrystals for catalytic cracking. *CrystEngComm* **2015**, *17*, 5680–5689. [[CrossRef](#)]
66. Lee, J.; Hong, U.G.; Hwang, S.; Youn, M.H.; Song, I.K. Production of light olefins through catalytic cracking of C₅ raffinate over carbon-templated ZSM-5. *Fuel Process. Technol.* **2013**, *108*, 25–30. [[CrossRef](#)]
67. Xiao, X.; Zhang, Y.; Jiang, G.; Liu, J.; Han, S.; Zhao, Z.; Wang, R.; Li, C.; Xu, C.; Duan, A.; et al. Simultaneous realization of high catalytic activity and stability for catalytic cracking of *n*-heptane on highly exposed crystal planes of nanosheet ZSM-5 zeolite. *Chem. Commun.* **2016**, *52*, 10068–10071. [[CrossRef](#)]
68. Tian, Y.; Zhang, B.; Liang, H.; Hou, X.; Wang, L.; Zhang, X.; Liu, G. Synthesis and performance of pillared HZSM-5 nanosheet zeolites for *n*-decane catalytic cracking to produce light olefins. *Appl. Catal. A* **2019**, *572*, 24–33. [[CrossRef](#)]
69. Zhang, X.; Cheng, D.-G.; Chen, F.; Zhan, X. The role of external acidity of hierarchical ZSM-5 zeolites in *n*-heptane catalytic cracking. *ChemCatChem* **2018**, *10*, 2655–2663. [[CrossRef](#)]
70. Ji, Y.; Shi, B.; Yang, H.; Yan, W. Synthesis of isomorphous MFI nanosheet zeolites for supercritical catalytic cracking of *n*-dodecane. *Appl. Catal. A* **2017**, *533*, 90–98. [[CrossRef](#)]
71. Khoshbin, R.; Oruji, S.; Karimzadeh, R. Catalytic cracking of light naphtha over hierarchical ZSM-5 using rice husk ash as silica source in presence of ultrasound energy: Effect of carbon nanotube content. *Adv. Powder Technol.* **2018**, *29*, 2176–2187. [[CrossRef](#)]
72. Vu, H.X.; Schneider, M.; Bentrup, U.; Dang, T.T.; Phan, B.M.Q.; Nguyen, D.A.; Armbruster, U.; Martin, A. Hierarchical ZSM-5 materials for an enhanced formation of gasoline-range hydrocarbons and light olefins in catalytic cracking of triglyceride-rich biomass. *Ind. Eng. Chem. Res.* **2015**, *54*, 1773–1782. [[CrossRef](#)]
73. Kim, W.-G.; So, J.; Choi, S.-W.; Liu, Y.; Dixit, R.S.; Sievers, C.; Sholl, D.S.; Nair, S.; Jones, C.W. Hierarchical Ga-MFI catalysts for propane dehydrogenation. *Chem. Mater.* **2017**, *29*, 7213–7222. [[CrossRef](#)]
74. Wannapakdee, W.; Yutthalekha, T.; Dugkhuntod, P.; Rodponthukwaji, K.; Thivasasith, A.; Nokbin, S.; Witoon, T.; Pengpanich, S.; Wattanakit, C. Dehydrogenation of propane to propylene using promoter-free hierarchical Pt/Silicalite-1 nanosheets. *Catalysts* **2019**, *9*, 174. [[CrossRef](#)]
75. Numpilai, T.; Wattanakit, C.; Chareonpanich, M.; Limtrakul, J.; Witoon, T. Optimization of synthesis condition for CO₂ hydrogenation to light olefins over In₂O₃ admixed with SAPO-34. *Energy Convers. Manag.* **2019**, *180*, 511–523. [[CrossRef](#)]
76. Gao, J.; Jia, C.; Liu, B. Direct and selective hydrogenation of CO₂ to ethylene and propene by bifunctional catalysts. *Catal. Sci. Technol.* **2017**, *7*, 5602–5607. [[CrossRef](#)]
77. Gao, P.; Dang, S.; Li, S.; Bu, X.; Liu, Z.; Qiu, M.; Yang, C.; Wang, H.; Zhong, L.; Han, Y.; et al. Direct production of lower olefins from CO₂ conversion via bifunctional catalysis. *ACS Catal.* **2017**, *8*, 571–578. [[CrossRef](#)]
78. Li, Z.; Wang, J.; Qu, Y.; Liu, H.; Tang, C.; Miao, S.; Feng, Z.; An, H.; Li, C. Highly selective conversion of carbon dioxide to lower olefins. *ACS Catal.* **2017**, *7*, 8544–8548. [[CrossRef](#)]
79. Dang, S.; Li, S.; Yang, C.; Chen, X.; Li, X.; Zhong, L.; Gao, P.; Sun, Y. Selective transformation of CO₂ and H₂ into lower olefins over In₂O₃-ZnZrO_x/SAPO-34 bifunctional catalysts. *ChemSusChem* **2019**, *12*, 3582–3591. [[CrossRef](#)]
80. Batamack, P.T.D.; Mathew, T.; Prakash, G.K.S. One-pot conversion of methane to light olefins or higher hydrocarbons through H-SAPO-34-catalyzed in situ halogenation. *J. Am. Chem. Soc.* **2017**, *139*, 18078–18083. [[CrossRef](#)]
81. Wen, D.; Liu, Q.; Fei, Z.; Yang, Y.; Zhang, Z.; Chen, X.; Tang, J.; Cui, M.; Qiao, X. Organosilane-assisted synthesis of hierarchical porous ZSM-5 zeolite as a durable catalyst for light-olefins production from chloromethane. *Ind. Eng. Chem. Res.* **2018**, *57*, 446–455. [[CrossRef](#)]
82. Liu, Q.; Wen, D.; Yang, Y.; Fei, Z.; Zhang, Z.; Chen, X.; Tang, J.; Cui, M.; Qiao, X. Enhanced catalytic performance for light-olefins production from chloromethane over hierarchical porous ZSM-5 zeolite synthesized by a growth-inhibition strategy. *Appl. Surf. Sci.* **2018**, *435*, 945–952. [[CrossRef](#)]

